Evaluating the Energy and Mechanical Properties of CSH/nano-CC Interface: An Atomic Investigation

Rongjia Wen[1], Qiang Zeng[1] and Boqing Gao[1]

[1] College of Civil Engineering and Architecture, Zhejiang University, Hangzhou 310058, PR China
Rongjia.wen@zju.edu.cn (Rongjia Wen), cengq14@zju.edu.cn (Qiang Zeng), bqgao@zju.edu.cn (Boqing Gao)

Abstract. *Carbonation of concrete generally leads to decalcification of calcium silicate hydrates (CSH) and generation of calcium carbonate (CC), however, the structure and mechanical properties of CSH-CC nano composites are far from being fully addressed. The CC formed by CSH carbonization mainly has three polymorphs, including calcite, vaterite and aragonite. Although different polymorphs have the same chemical composition, they belong to different crystal systems and have completely different unit cell structures. In this paper, the CSH and three polymorphs nano-CC are constructed at the atomic level, and the interface properties between them are explored by reactive molecular dynamics (MD) simulations. The results show the greater interfacial bonding energy, the better the mechanical properties of the CSH-CC composite. Moreover, interface transition region (ITR) emerges between CSH and CC polymorphs, and the ITR thickness is different. The atomic structure in ITR is different from that in the middle region, the former is more disorderly and the coordination number in ITR is significantly reduced, thus showing a metastable state. The findings would deepen the mechanistic understanding of interface properties between CSH and nano-CC.*

Keywords: *Calcium Silicate Hydrate, Nano-calcium Carbonate, Interface Properties, Reactive Molecular Dynamics.*

1 Introduction

The crystalline calcium carbonate (CC) formed by the carbonization of calcium silicate hydrates (CSH) mainly has three different polymorphs, including calcite, vaterite and aragonite. The proportion of CC polymorphs by carbonization varies with Ca/Si ratio (Kangni-Foli *et al.*, 2021). Carbonation of CSH with high Ca/Si ratios (more than 1.0) usually generates calcite, probably because the excess calcium ions in CSH are more likely to balance the negatively charged calcite surface (Black *et al.*, 2007). However, aragonite and vaterite are more likely to be formed for CSH with Ca/Si ratio less than 0.67, and between 0.67 and 1.0, respectively. Although different CC polymorphs have the same chemical composition, they belong to different crystal systems (hexagonal vaterite, orthorhombic aragonite, and rhombohedral calcite (Niu *et al.*, 2022)) and have completely different unit cell structures. At present, the interfacial interactions between different polymorphs and CSH at the atomic scale have not been fully revealed.

In this work, the CSH and nano-CC polymorphs were constructed at the atomic level, and the interface properties between them were explored by reactive molecular dynamics (MD) simulations. Specifically, the interface structure and mechanical properties of the composites were analyzed by various mathematical means.

2 Methodology

2.1 Modeling Process

Firstly, a CSH supercell (4×3×1) was constructed based on the Hamid's tobermorite with a layer spacing of 11 Å (a = 22.317 Å, b = 22.170 Å, c = 22.770 Å, α = 90°, β = 90 °, γ = 90 °), the silicon chain was broken by removing the partially neutral SiO_2 (located in the bridged silicon-oxygen tetrahedron) to meet the measured Q_n distribution ($Q_0 = 0$, $Q_1 = 0.6$, $Q_2 = 0.4$). Subsequently, the Monte Carlo method was performed to absorb water molecules and calcium ions into the above-mentioned model (between calcium-silicon layers) to satisfy the measured Ca/Si ratio and H_2O/Si ratio (1.7 and 1.3, respectively). This CSH model has a total of 180 calcium atoms, of which 96 are interlayer calcium and 84 are intralayer calcium. At the same time, some hydroxyl groups were also absorbed to balance the charge. The final CSH model contains 40 dimers, 20 pentamers and 2 octamers, that is, dimers account for 64.5%, in line with the results reported for fresh cement (about 60%). In addition, the density is about 2.654 g/cm^3, and the average chain length (MCL) is about 3.3. The data are close to those in previous report (Kunhi Mohamed *et al.*, 2018).

Since both CSH gel and CC crystal are anisotropic materials at the nanoscale, the mechanical properties of CSH-CC may differ greatly when they are connected by different surfaces. For CSH gel, the (001) surface with lowest interface energy was selected (Jamil, Javadi and Heinz, 2020); while for three polymorphs CC, their most typical dissociation surfaces were selected (the (104) surface of calcite (Jiang, Zhao and Xu, 2016), the (010) surface of aragonite (Zhang, Hong and Chen, 2019), and the (100) surface of vaterite (X. Wang *et al.*, 2017)). The above models were extended and orthogonalized to make their lattice parameters match as much as possible. Finally, the model of CSH and CC were connected, leaving a gap of 1 Å in between (Sekkal and Zaoui, 2017).

2.2 Force Field

The ReaxFF (Duin *et al.*, 2001) is a potential function based on bond order, and its energy expression is shown in Eq. 1. Bond order is determined step by step from the distance between atoms to evaluate bond dissociation and formation, and to further analyze the forces generated by non-bond interactions. The valence electron energy and torsion angle energy related to the bond order gradually disappears during bond dissociation. Non-bond interactions, such as van der Waals energy and Coulomb energy, are considered between each atom pair. In addition, the electronegativity equalization method (EEM) is used to calculate the atomic charge. Therefore, compared with the classical ClayFF (Cygan, Liang and Kalinichev, 2004), ReaxFF consumes more computing resources, but it can describe the dissociation and formation of chemical bonds. In this paper, the ReaxFF was used to investigate the energy and structure of three different CSH-CC interface in this paper. The parameters related to C are derived from the metal carbonate force field (Dasgupta, Chen and Van Duin, 2022), and the other parameters are based on the clay-zeolite force field (Pitman and Van Duin, 2012).

$$E_{sys} = E_{bo} + E_{over} + E_{under} + E_{va} + E_{to} + E_{lp} + E_{vd} + E_{co} \qquad (1)$$

where, E_{sys} is the total energy of system; E_{over} and E_{under} are the energy penalty for over- and under-coordination of atoms, respectively; E_{bo}, E_{va}, E_{to}, E_{lp}, E_{vd} and E_{co} are the bond energy,

valence angle energy, torsion angle energy, lone pair energy, Van der Waals energy and Coulomb energy, respectively.

2.3 Simulation Detail

MD simulation was carried out in lammps software. First, the temperature was gradually increased from 300 K to 600 K to break through the energy barrier that inhibits structural relaxation. After that, at a constant pressure and temperature (NPT ensemble, 300 K, 1 atm), the final equilibrium state was then reached by further relaxation of 400 ps. The time step was set as 0.25fs, the trajectory integral was run by velocity-verlet algorithm, and the temperature and pressure were controlled by Nosé-Hoover algorithm. The whole system was gradually stretched along the Z direction at a rate of 0.01/ps to study the mechanical response of the CSH-CC systems with three different polymorphs. During the tensile process, the pressure in the X and Y directions was set to 0 to consider the Poisson effect.

3 Results and Discussion

3.1 Energy and Mechanical Properties

After the CSH was cut in half along interlayer (001 direction), the number of calcium ions on the two surfaces of CSH is different (Figure 1a) due to the random distribution of interlayer calcium ions (Ca_w). A-surface has 92 calcium ions, while b-surface has 76. Figure 1b shows that the interfacial bonding energy of vaterite is not sensitive to the number of surface calcium ions. The calcite and the a-surface (contains more surface calcium ions) can produce stronger interfacial bonding energy; on the contrary, aragonite has a strong interfacial bonding energy with the b-surface. The reason for these phenomena is related to the atomic density distribution (analyzed in section 3.2). In addition, the order of total interfacial bonding energy is: aragonite > calcite > vaterite, in keeping with the order of tensile strength of CSH-CC (Figure 1c). This shows that the greater interfacial bonding energy, the better the mechanical properties of the CSH-CC composite.
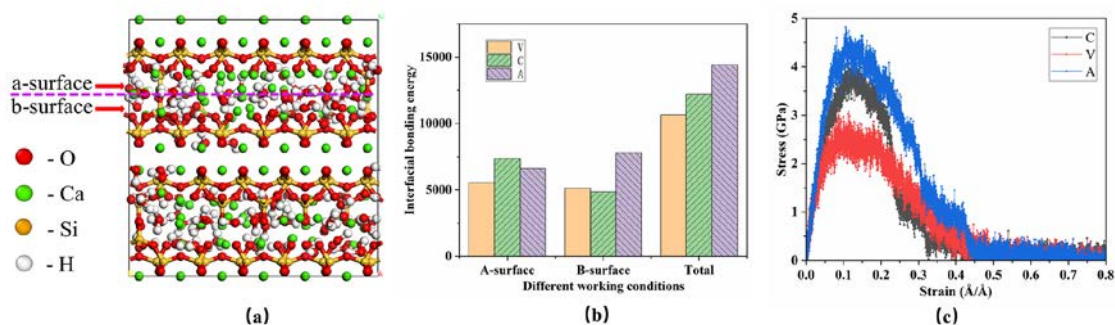

Figure 1. (a) Cutting crystal surface; (b) Interfacial bonding energy and (c) mechanical properties of CSH-CC.

3.2 Atomic Local Structure

The atomic structure distribution shows that interface transition region (ITR) emerges between CSH and CC polymorphs, and the ITR thickness is different: vaterite (10 Å) > calcite (8 Å) > aragonite (5 Å). For calcite (Figure 2b), the density peak of carbonate is closer to the surface than calcium in CC (Ca_c), so calcite has a strong interaction with surface Ca ions. This is the reason why calcite can produce stronger interfacial bonding energy with a-surface. The results of first-principles simulation (Wang *et al.*, 2017) found that, in the surface of calcite, Ca moves inward and carbonate moves outward to achieve the lowest surface energy. This is consistent with the MD results in this paper, and may be the main reason for the negative ζ potential on calcite surface. In contrast, for aragonite (Figure 2c), the density peak of Ca_c is closer to the surface than that of carbonate, so it has better interaction with the silicon chain in CSH. However, for vaterite (Figure 2a), the ion peak in ITR becomes more disordered, with no apparent preference. In addition, part of Ca_c in aragonite can dissociate into the interface (see Figure 2c, more calcium ion enrichment can be observed at the surface), playing a good bridging interaction, so the total interfacial bonding energy of aragonite is the largest in the three CSH-CC systems.
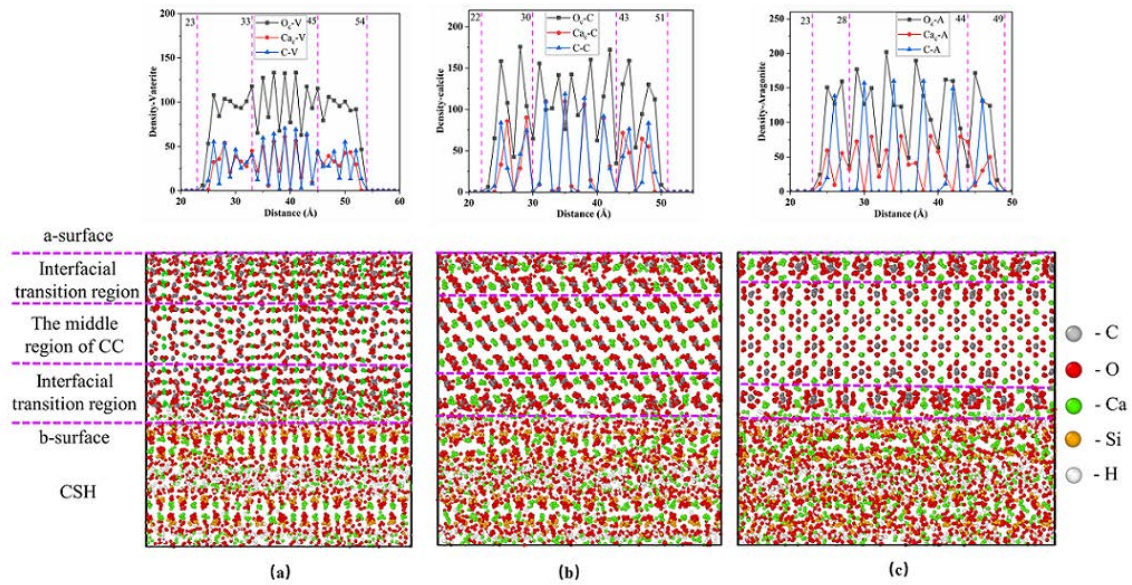
Figure 2. Atomic structure distribution of (a) vaterite, (b) calcite and (c) aragonite

The first peak of RDF in figure 3 represents the equilibrium bond length of corresponding ion pair (AI, CI and VI represent the ITR of aragonite, calcite and vaterite, the same as the following). Figure 3a shows that for Ca_c-O_c, the equilibrium bond length in ITR is slightly different from that in the middle region (calcite and aragonite shorten 1%, while vaterite increases 1%). However, the bond length of the C-O_c covalent bond remains unchanged in each region (Figure 3b). Figures 3d, e, and f are angular correlation functions (ADF) for three polymorphs, respectively. A_a and A_b represent the ITR of aragonite near the a-surface and b-surface respectively and A_m represents the middle region of aragonite. Other polymorphs are

the same. In the middle region of aragonite, the angle between the C-O_c bond and the Z axis (Figure 3c) is basically 0°, 60°, and 120°. In the ITR, the intensity of above peaks decrease somewhat, and there are some small peaks form between these main peaks. Figure 3e shows that calcite has only two main peaks in the middle region, 60° and 120° respectively. Because it is carbonate ions in the outermost layer in calcite, the angle distribution is affected by the surface calcium ions of CSH. For a-surface, the intensity of peak at 60 ° decreases, while for b-surface, the intensity of peak at 120° decreases. For vaterite (Figure 3f), the peaks in the middle region are at 30°, 90° and 150°, respectively, while for the ITR, there is only a peak at 90°. From RDF and ADF, it can be concluded that the atomic structure of ITR has changed under the influence of CSH.
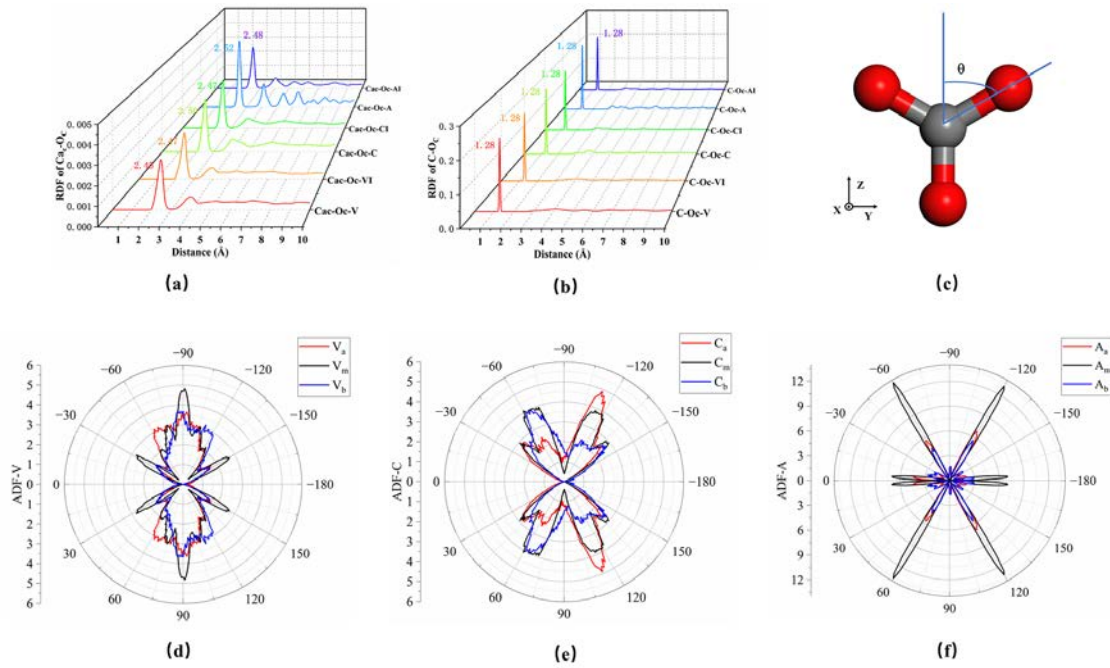
Figure 3. RDF of (a) Ca_c-O_c and (b) C-O_c; (c) Angle calculated in ADF; ADF of (d) vaterite, (e) calcite and (f) aragonite

3.3 Atomic Dynamic Characteristics

Figure 4a shows that the MSD value of Ca_c in the ITR of aragonite is the largest among all atoms, indicating that Ca_c is the most active, so it is easier to dissociate into the interface area. For calcite, the opposite phenomenon is observed, the carbonate in the ITR is the most active. These phenomena indicate that the outermost atoms are generally more active. However, for vaterite (Figure 4a), the MSD of atoms in different regions is not obviously different. Moreover, the MSD of vaterite in the middle region is significantly greater than that of calcite and aragonite. Therefore, consistent with previous reports (Liu *et al.*, 2022), vaterite is the most thermodynamically unstable among three polymorphs. In contrast, the MSD value of the atoms in calcite is the smallest, so it is the most stable.
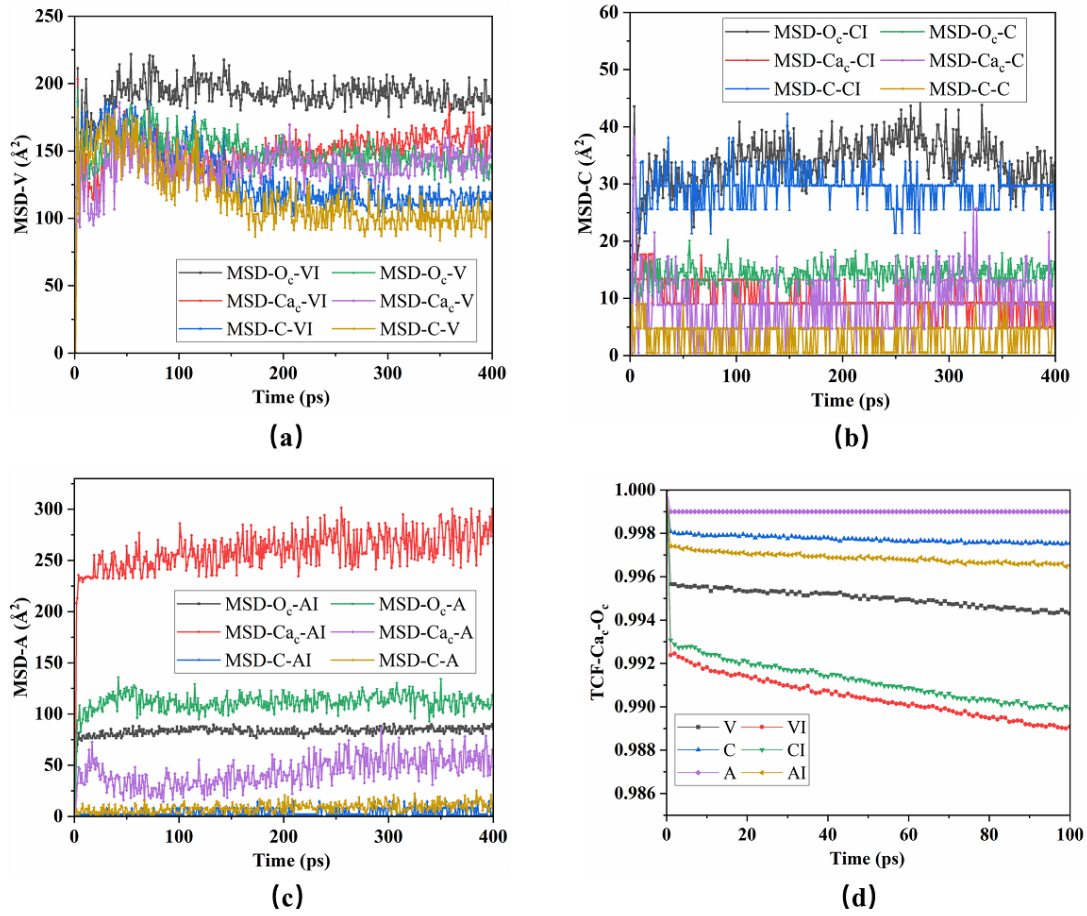
Figure 4. MSD of (a) vaterite, (b) calcite and (c) aragonite; (d) TCF of Ca_c-O_c.

Table 1. Coordination number of vaterite, calcite and aragonite

	A_a	A_m	A_b	C_a	C_m	C_b	V_a	V_m	V_b
Ca_c-O_c	6.553	8.321	6.738	7.207	7.976	7.086	6.701	7.082	6.692
C-O_c	2.992	2.950	2.854	2.889	2.922	2.871	2.918	2.922	2.846

Table 1 shows that the coordination number (CN) of Ca_c-O_c ionic bonds in the ITR decreases, and this phenomenon is more obvious for calcite and aragonite. Usually, the higher the CN of atoms, the more stable it is (Huang *et al.*, 2015). Therefore, in ITR, the stability of Ca_c-O_c ionic bond decreases, which can also be reflected from time correlation function (TCF) (Figure 4d, the larger the area enclosed by TCF and X axis, the more stable the corresponding chemical bond). It is worth noting that in the ITR, the CN of Ca_c-O_c in aragonite is larger in a-surface than in b-surface; the opposite is true for calcite; and the vaterite is almost equal. This proves again that they have different sensitivities to surface calcium ions. However, the C-O_c covalent bond is very stable, so its CN remains almost unchanged in different regions.

4 Conclusions

In this paper, reactive molecular dynamics simulations were used to investigate the interface structure and mechanical properties of calcium silicate hydrate and three polymorphs nano-calcium carbonate composites. The major conclusions can be summarized as follows:

1. The interfacial interaction energy between calcium silicate hydrate and aragonite is greater than that of calcite and vaterite (aragonite > calcite > vaterite). The mechanical properties of the composite system also show the same order. This signifies that the greater interfacial bonding energy, the better the mechanical properties of the calcium silicate hydrate and calcium carbonate composites.

2. Interface transition region emerges between calcium silicate hydrate and three different calcium carbonate polymorphs, and its thickness is different: vaterite (10 Å) > calcite (8 Å) > aragonite (5 Å). Moreover, the surface of different polymorphs has different sensitivity to the surface calcium ions of calcium silicate hydrate. Calcite can produce higher interfacial interaction energy with the surface with more calcium ions, while aragonite is the opposite.

3. The atomic structure in interface transition region is different from that in the middle region, the former is more disorderly and the coordination number in interface transition region is significantly reduced, thus showing a metastable state. At the same time, time correlation function also shows that the ionic bond strength in interface transition region is reduced. This indirectly indicates that when carbonate is deposited on the surface of calcium silicate hydrate, amorphous calcium carbonate rather than regular calcium carbonate crystals may be formed first.

References

Black, L., Breen, C., Yarwood, J., Garbev, K., Stemmermann, P. and Gasharova, B. (2007). *Structural features of C-S-H(I) and its carbonation in air-A Raman spectroscopic study. Part II: Carbonated phases*, Journal of the American Ceramic Society, 90(3), 908–917.

Cygan, R.T., Liang, J. and Kalinichev, A.G. (2004). *Molecular Models of Hydroxide , Oxyhydroxide , and Clay Phases and the Development of a General Force Field*, The Journal of Physical Chemistry B, 108(4), 1255–1266.

Dasgupta, N., Chen, C. and Van Duin, A.C.T. (2022). *Development and application of ReaxFF methodology for understanding the chemical dynamics of metal carbonates in aqueous solutions*, Physical Chemistry Chemical Physics, 24(5), 3322–3337.

Duin, A.C.T. Van, Dasgupta, S., Lorant, F. and Iii, W.A.G. (2001). *ReaxFF: A Reactive Force Field for Hydrocarbons*, The Journal of Physical Chemistry A, 105, 9396–9409.

Huang, L.F., Grabowski, B., Mceniry, E., Trinkle, D.R. and Neugebauer, J. (2015). *Importance of coordination number and bond length in titanium revealed by electronic structure investigations*, Physica Status Solidi (B) Basic Research, 252(9), 1907–1924.

Jamil, T., Javadi, A. and Heinz, H. (2020). *Mechanism of molecular interaction of acrylate-polyethylene glycol acrylate copolymers with calcium silicate hydrate surfaces*, Green Chemistry, 22(5), 1577–1593.

Jiang, J., Zhao, J. and Xu, Y. (2016). *Molecular simulations and critical pH studies for the interactions between 2-phosphonobutane-1,2,4-tricarboxylic acid and calcite surfaces in circular cooling water systems*, Desalination and Water Treatment, 57(5), 2152–2158.

Kangni-Foli, E., Poyet, S., Le Bescop, P., Charpentier, T., Bernachy-Barbé, F., Dauzères, A., L'Hôpital, E. and d'Espinose de Lacaillerie, J.B. (2021). *Carbonation of model cement pastes: The mineralogical origin of microstructural changes and shrinkage*, Cement and Concrete Research, 144(November 2020).

Kunhi Mohamed, A., Parker, S.C., Bowen, P. and Galmarini, S. (2018). *An atomistic building block description of C-S-H - Towards a realistic C-S-H model*, Cement and Concrete Research, 107(March), 221–235.

Liu, X., Feng, P., Cai, Y., Yu, X., Yu, C. and Ran, Q. (2022). *Carbonation behavior of calcium silicate hydrate (C-S-H): Its potential for CO2 capture*, Chemical Engineering Journal, 431, 134243.

Niu, Y.Q., Liu, J.H., Aymonier, C., Fermani, S., Kralj, D., Falini, G. and Zhou, C.H. (2022). *Calcium carbonate: controlled synthesis, surface functionalization, and nanostructured materials*, Chemical Society Reviews, 51(18), 7883–7943.

Pitman, M.C. and Van Duin, A.C.T. (2012). *Dynamics of confined reactive water in smectite clay-zeolite composites*, Journal of the American Chemical Society, 134(6), 3042–3053.

Sekkal, W. and Zaoui, A. (2017). *Enhancing the interfacial bond strength of cement nanocomposite with carbonate nanostructure*, Composites Part B: Engineering, 124, 111–119.

Wang, Ji., Qin, Z., Yue, Q., Long, L., Jun, Y. and Wei, C. (2017). *The first principles of the crystal structure and active sites of calcite*, Chinese Journal of Engineering, 39(4), 487–493.

Wang, X., Sun, X., Zhang, Q., Marchetti, A., Wu, L. and Guan, Y. (2017). *Hierarchical pine-dendritic vaterite preparation and micropatterning with microwave technique*, Materials Letters, 208, 39–42.

Zhang, N., Hong, Y. and Chen, Y. (2019). *Dynamic crack propagation behaviors of calcium carbonate: aragonite*, Journal of Materials Science, 54(4), 2779–2786.